Available online at www.sciencedirect.com
SCIENCE DIRECT®
Journal of Photochemistry and Photobiology A: Chemistry 157 (2003) 211–222
Journal of Photochemistry and Photobiology A:Chemistry
www.elsevier.com/locate/jphotochem

Measurements of the infrared absorption cross-sections of haloalkanes and their use in a simplified calculational approach for estimating direct global warming potentials

Vladimir L. Orkin [a,b,*], Andrey G. Guschin [a], Igor K. Larin [a], Robert E. Huie [b], Michael J. Kurylo [b]

[a] *Institute of Energy Problems of Chemical Physics, Russian Academy of Sciences, Leninsky Prospect 38, Bldg. 2, Moscow 117829, Russia*
[b] *Physical and Chemical Properties Division, National Institute of Standards and Technology, Gaithersburg, MD 20899, USA*

Received 18 June 2002; received in revised form 14 September 2002; accepted 14 September 2002

Abstract

The infrared absorption cross-sections and integrated band intensities (IBIs) for 21 haloalkanes: $CFCl_3$, CF_2Cl_2, CF_2Br_2, CH_2F_2, CHF_2Cl, CHF_2Br, CF_3Br, $CHCl_2$–CF_2Cl, $CHFCl$–$CFCl_2$, $CHCl_2$–CF_3, $CHClBr$–CF_3, $CHFCl$–CF_2Cl, $CHFBr$–CF_3, CHF_2–CF_3, CH_2Br–CF_3, CH_2F–$CFCl_2$, CH_2F–CF_3, CH_3–CCl_3, CH_3–$CFCl_2$, CH_3–CF_2–CF_3, and CHF_2–CH_2–CF_3 were measured over the wavenumber range 400–1600 cm^{-1} at $T = 295$ K. The effect of air pressure on measured spectra was also investigated. These results are used to demonstrate a simple calculational approach for estimating the direct global warming potentials (GWPs) of such chemicals. The results obtained are compared with those derived from more comprehensive atmospheric modeling calculations appearing in the literature.

Keywords: Infrared absorption cross-sections; Pressure broadening; CFC; Halon; Infrared forcing; Global warming potential

1. Introduction

The recognition that anthropogenic gases can have global effects, such as ozone depletion and greenhouse warming, has fostered scientific analyses of the effects of industrial emissions on our atmospheric environment. The production of the main industrial ozone destroying compounds (i.e. chlorofluorocarbons (CFC) and halons) is now restricted by national and international agreements, while alternative substances are under careful examination. There are presently no regulations in effect with respect to the production of substances that can cause climate change. Nevertheless, concern about the possible role of new industrial products as greenhouse gases has led to interest in evaluating their infrared absorption and atmospheric lifetimes.

Global warming potentials (GWPs) have been adopted as convenient parameters to quantify the relative contributions of various gases to global warming using either CFC-11 ($CFCl_3$) or CO_2 as a reference gas [1,2]. The GWP of a gas depends on its ability to absorb the Earth's outgoing infrared radiation and its residence time in the atmosphere. All halogen-containing hydrocarbons are infrared active gases because of their strong absorption bands in the region of the atmospheric transparency window between ca. 8 and 12 μm. Coupled radiative-chemical two- and three-dimensional models of the atmosphere are generally used to calculate GWPs over different time horizons.

The atmospheric lifetimes of most hydrogen-containing halocarbons that are in use or considered for use as CFC and halon replacements can be easily estimated from the rate constants of their reactions with hydroxyl radicals. In this simplified procedure, the reactivity is compared with that of methyl chloroform (MC) whose atmospheric lifetime is well established [3–5]. In this paper, we extend this relative approach to the estimation of the GWPs based on measured infrared absorption cross-sections and the measured spectrum of the Earth's outgoing radiation.

Radiative transfer models of the atmosphere that are used for global climate related calculations generally utilize an infrared radiation pattern averaged over spectral intervals of a few cm^{-1} and wider. Therefore, they really do not require high-resolution IR absorption spectra of the trace gases under investigation. Nevertheless, it is important to have correctly determined integrated absorption line intensities (absorption band intensities) that

* Corresponding author.
E-mail address: vladimir.orkin@nist.gov (V.L. Orkin).

1010-6030/03/$ – see front matter © 2003 Elsevier Science B.V. All rights reserved.
doi:10.1016/S1010-6030(03)00057-1

are free of errors associated with inadequate instrumental resolution.

In the present paper we report results of our IR absorption measurements for 17 partially halogenated hydrocarbons that are being used or have been proposed as CFC and halon replacements as well as for CFC-11, CFC-12 (CF_2Cl_2), Halon-1301 (CF_3Br), and Halon-1202 (CF_2Br_2). The effect of an inert gas on the measured absorption band intensities was investigated for all compounds. Direct GWPs of these chemicals were then derived. The technique described in the present paper has been used to estimate GWPs in several of our previous studies [6–9].

2. Experimental procedures[1]

The spectra of halogenated methanes and ethanes were obtained with a Specord M-80 double beam diffraction spectrophotometer coupled to a computer for numeric data collection and analysis. All the data presented were measured with a 0.5 cm^{-1} spectral slit width at 0.2 cm^{-1} increments. Spectral slit widths of 1.0 and 2.5 cm^{-1} were used in test experiments to check if the measured absorption band intensities depended on the slit width. Photometric noise was ca. 0.007 absorption units during these experiments. The 12.16 ± 0.03 cm glass absorption cell fitted with KBr windows was fixed in the spectrophotometer to prevent a baseline shift. Between measurements the cell was pumped out down to ca. 0.1 Pa and then filled with the gas to be studied. This procedure was repeated two to three times for each gas to ensure the sample purity in the cell. The temperature of the cell was $T = 295 \pm 1$ K.

The spectra of fluorinated propanes, $CHF_2CH_2CF_3$ and $CH_3CF_2CF_3$ were obtained with a Fourier transform spectrophotometer Bruker IFS-66v equipped with a 20.15 ± 0.05 cm long absorption cell fitted with KBr windows, also at a temperature $T = 295 \pm 1$ K. The data presented here for these two compounds were obtained with ca. 0.12 cm^{-1} spectral resolution. A few additional test experiments were performed at this higher spectral resolution for CHF_2Cl, CHF_2CF_3, CH_2FCF_3, CH_3CFCl_2, CF_2Br_2, and CH_2F_2.

Sample pressures were measured by using a bellows inductive manometer in the range 0–300 Torr (0–40 kPa) with a precision of ca. ±0.01 Torr (±1 Pa) and a mechanical manometer in the range of 200–700 Torr (27–93 kPa). The absolute calibration of each was periodically checked by measuring water vapor pressure at its melting point, P_{H_2O} ($T = 273$ K) = 4.58 Torr (610.5 Pa). The linearity of the manometer was checked as well. Full scale 10 and 1000 Torr MKS Baratron manometers were used in the higher resolution measurements.

Samples of the halogenated methanes and ethanes used in this study were provided by the State Institute of Applied Chemistry in St. Petersburg, Russia, with the stated purities: $CFCl_3$ (>99.9%), CF_2Cl_2 (>99.8%), CF_2Br_2 (ca. 98% with $CFCl_3$ as the main impurity), CH_2F_2 (>99.9%), CHF_2Cl (>99.9%), CHF_2Br (>99.8%), $CHCl_2CF_2Cl$ (>99.6%), $CHFClCFCl_2$ (>98.3%, the $CHCl_2CF_2Cl$ isomer being the main impurity), $CHCl_2CF_3$ (>99.7%), $CHClBrCF_3$ (>99.9%), $CHFClCF_2Cl$ (>99.9%), $CHFBrCF_3$ (>99.7%), CHF_2CF_3 (>99.9%), CH_2BrCF_3 (>99.9%), CH_2FCF_3 (>99.9%), CH_3CCl_3 (>99.9%), CH_3CFCl_2 (>99.9%); and from the Institute of Chemical Technology in Moscow, Russia, with the stated purities: $CHFClCFCl_2$ (>99.7%), CH_2FCFCl_2 (>99.9%), CH_3CFCl_2 (>99.9%). An additional sample of CH_2FCF_3, provided by the Oak Ridge National Laboratory under subcontract 86-SL103 (made by du Pont de Nemours & Co., >99.9%), was studied as well. The sample of $CHF_2CH_2CF_3$ was provided by Allied-Signal Corp., who found no impurities using both GC-MS and GC-FID techniques with a detection limit of better than 1 ppm. The original sample of $CH_3CF_2CF_3$ obtained from PCR Corp. was purified as described by Orkin et al. [10] to better than 99.98%. All samples were subjected to vacuum distillation before measurements to eliminate possible volatile impurities, mainly nitrogen, oxygen, carbon dioxide. Air was purified by passage through a liquid nitrogen trap before the experiments.

As noted above, all of the samples (with the exception of CF_2Br_2 and $CHFClCFCl_2$) had purities exceeding 99.5%. Therefore, all absorption bands with integrated intensities exceeding 0.5% of the strongest band were considered to be absorption bands of the compound under study. The measured spectra of CF_2Br_2 and $CHFClCFCl_2$ were corrected slightly using the measured spectra of main impurities ($CFCl_3$ and $CHCl_2CF_2Cl$, respectively).

Absorption spectra of the evacuated cell and the cell filled with the chemical under study were recorded sequentially to calculate the absorption cross-sections from their differences at different concentrations, using the Beer–Lambert law:

$$\sigma(\nu) = \frac{2.303}{[\mathrm{HHC}] \times L}(A_{\mathrm{HHC}}(\nu) - A_0(\nu)) \quad (1)$$

where $\sigma(\nu)$ is the absorption cross-section at wavenumber ν (cm^2 $molecule^{-1}$); $A_{\mathrm{HHC}}(\nu)$ and $A_0(\nu)$ the absorbancies (base 10) in the presence of the hydrohalocarbon of interest and of the evacuated cell at wavenumber ν, respectively; [HHC] the concentration of hydrohalocarbon (molecule cm^{-3}); and L is the optical path length (cm). The spectrum of each absorption band was recorded at 5–9 different hydrohalocarbon pressures suitable for that band such that the maximum absorbance did not exceed $A_{\mathrm{HHC}}(\nu) = 1.0$. Linear least-square fits were applied to the results of absorption measurements at various sample pressures in order to obtain absorption cross-sections as well as

[1] Certain commercial equipment, instruments, or materials are identified in this article in order to adequately specify the experimental procedure. Such identification does not imply recognition or endorsement by the National Institute of Standards and Technology, nor does it imply that the material or equipment identified are necessarily the best available for the purpose.

integrated band intensities (IBIs). The overall instrumental error associated with the path length, pressure measurements, temperature stability, and measured absorbance was estimated to be less than 2% for the strong absorption bands.

3. Results and discussion

3.1. Pressure broadening study

Rotational structure in the IR spectrum can cause an error in determining an integrated band strength because of the lack of adequate spectral resolution of the spectrophotometer. A high pressure of a non-absorbing gas can be used for line broadening to reduce or eliminate the rotational structure when the rotational spacing is not very wide. The pressure broadening technique was introduced and carefully described by Wilson and Wells [11] and has been successfully employed for infrared intensity measurements [12].

Nevertheless, in the majority of studies of infrared intensities of CFCs and their proposed replacements, either no broadening gas or one atmosphere of dry air or nitrogen has typically been used to pressurize a sample. There are results from two research groups only [13–17] in which the effect of inert gas pressure was checked. Roehl et al. [13] measured absorption spectra of C_1–C_6 perfluoroalkanes with a spectral resolution of 0.02 and 1 cm^{-1}. The authors mentioned an effect of the instrumental resolution and the nitrogen pressure (below 200 Torr, 27 kPa) on the measured band intensities in the case of CF_4, but did not report this information quantitatively. Newnham and Ballard [14], Newnham et al. [15], Smith et al. [16,17] studied some CFC substitutes with high-resolution (0.03 and 0.002 cm^{-1}). These studies illustrated changes in high-resolution IR spectra of halogenated alkanes due to the broadening effect of an inert gas. Smith et al. [17] found no changes in the measured band intensities when pressurizing samples of HFC-134 (CHF_2CHF_2) and HFC-143a (CH_3CF_3) with dry synthetic air up to 100 kPa. Earlier, the same group [16] reported a decrease in the absorption band intensities (11 and 18%) when CH_2F_2 (HFC-32) was pressurized with 750 Torr (100 kPa) of dry air. This observation is probably due to some experimental artifact since the collisional line broadening should cause only a redistribution of the intensity in the absorption line, while the IBI should remain the same. The magnitude of any possible error in the measured spectrum caused by the inadequate spectral resolution of the instrument depends on both the instrumental resolution itself and the nature of the spectrum of the studied compound under the specific conditions of pressure and temperature. Generally speaking, the effect of pressure broadening should always be investigated to be sure that the measured IBI does not depend on either sample or total gas pressure.

In the present study, spectra were recorded for both an undiluted (pure) hydrohalocarbon sample and one in the presence of 87 kPa (650 Torr) of dry air. No differences in the IBIs were obtained except for CHF_2Cl (HCFC-22) and CH_2F_2 (HFC-32). HCFC-22 showed a 12% increase in the total IBI over the range 700–1400 cm^{-1} when pressurized by either 13 or 87 kPa (100 or 650 Torr) of air. The broadening effect was different for different spectral features. For example, the measured absorption over the main absorption band (1050–1200 cm^{-1}) increased by 8–9% when pressurized by either air or CO_2, while the 1 cm^{-1} wide band centered at the narrow absorption peak 829.1 cm^{-1} increased by about 25%. The band intensities reported for these compounds in Tables 2 and 3 were obtained from pressure-broadened spectra.

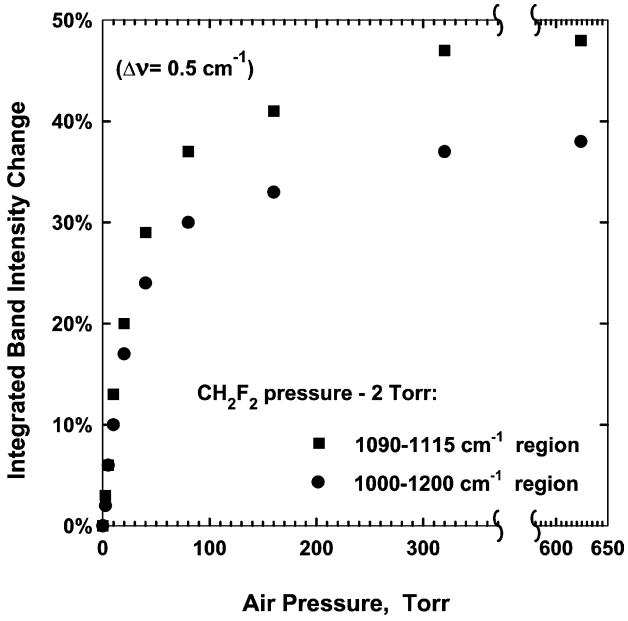

Fig. 1. The relative change of measured band intensities of CH_2F_2 (HFC-32) vs. broadening air pressure. The band intensity measured with 2 Torr (0.27 kPa) of HFC-32 without air is the reference. Band intensities were measured over 1000–1200 cm^{-1} (circles) and 1091–1114 cm^{-1} (squares) intervals with the 0.5 cm^{-1} spectral resolution.

The most pronounced effect of gas pressure was found in the case of CH_2F_2 (HFC-32). Fig. 1 shows relative changes in the IBIs for both the entire 1000–1200 cm^{-1} band and for its highest unresolved "peak" (1114.4–1090.8 cm^{-1}) when 2.0 Torr (0.27 kPa) of CH_2F_2 was pressurized by air. As mentioned earlier, the spectrum of CH_2F_2 was also obtained with a higher spectral resolution of ca. 0.12 cm^{-1} and recorded with a step of 0.06 cm^{-1} using a Fourier transform spectrometer Bruker IFS-66v. In all cases the band intensities increase with increasing air pressure and become pressure independent within the pressure range of our measurements. It is not very surprising that difluoromethane manifested such a dependence of IBI on broadening gas pressure. CH_2F_2 contains only two relatively heavy F atoms and thus has the lowest density of vibrational–rotational transitions (i.e. lowest density of corresponding absorption lines in the spectrum) among the substances in this study.

Fig. 2a shows "resolved" spectra of CH_2F_2 (2 Torr of pure sample diluted with air at various total pressures) over 1098–1105 cm^{-1} obtained with 0.12 cm^{-1} spectral resolution. As can be seen, the absorption intensity increases with air pressure in the cell while line broadening results in "smoothing" of the spectral features. One can see the spectrum evolution with increasing pressure from Fig. 2b, which is a transformation of Fig. 2a. It shows the structure of spectra ratios obtained at 270 Pa of CH_2F_2 and various air pressures referenced to that of the undiluted 270 Pa CH_2F_2 sample. The original spectrum of undiluted sample is shown as well to indicate the positions of the peaks for comparison. The rotational structure is not completely resolved due to the spectral resolution of the spectrophotometer. Nevertheless, it is clear that pressure broadening is the cause of the spectral smoothing. The spectra ratio increases uniformly at low air pressure (the structure of the ratio is not very pronounced at 2.7 and 14.7 kPa of air). At higher pressure (between 14.7 and 100 kPa of air), the average absorption remains stable while there is an increased absorption in the spectral valleys because of line overlapping. This is consistent with spectrum broadening by the inert gas. Initially, broadening of the narrow absorption lines results in an increase in the measured line intensities. Further broadening then results in the line overlapping and causes the actual structure to disappear (i.e. a smoothing of the spectrum). Smith et al. [16] measured the IR spectrum of CH_2F_2 (at a sample pressure of 100–150 Pa) with the spectral resolution of 0.03 cm^{-1} and studied the effect of pressure broadening. Their results also illustrate the disappearance of the rotational structure in the CH_2F_2 absorption band near 1100 cm^{-1} when the sample was pressurized with 100 kPa of dry synthetic air.

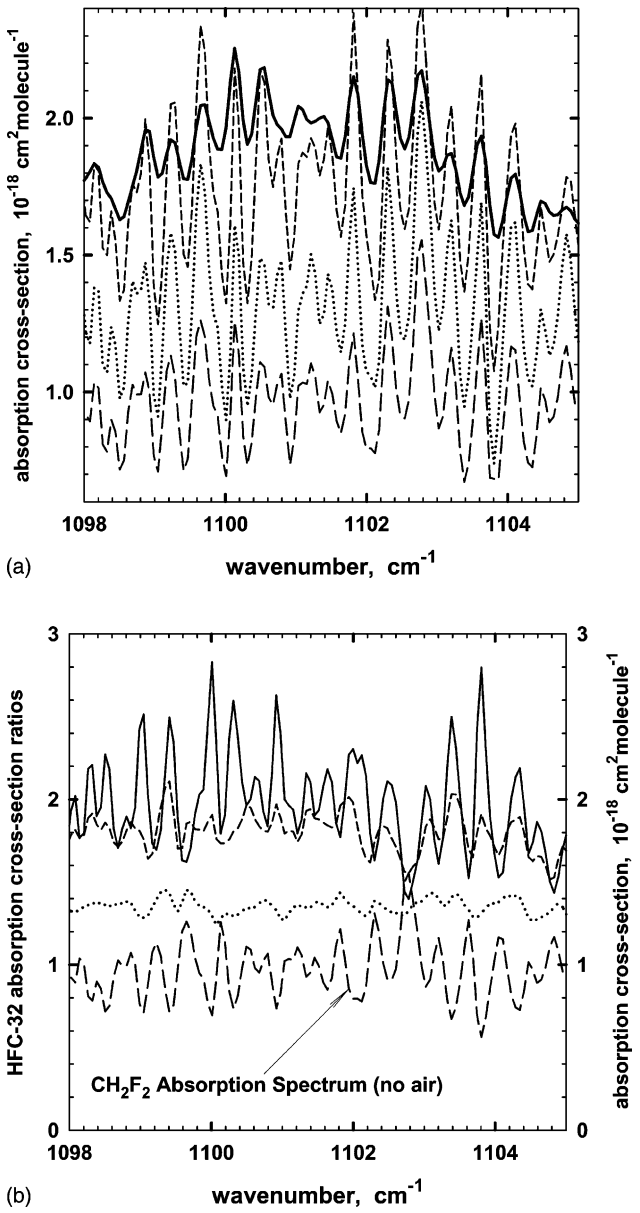

Fig. 2. (a) The evolution of the measured 1098–1105 cm^{-1} absorption band of CH_2F_2 with broadening air pressure. Spectra were obtained with 0.12 cm^{-1} spectral resolution at 0.27 kPa (2 Torr) of CH_2F_2 pressurized with air up to 2.7 kPa (20 Torr: dotted line), 14.7 kPa (110 Torr: short dashed line), and 100 kPa (750 Torr: solid line). The spectrum of 0.27 kPa (2 Torr) of pure CH_2F_2 is shown by the long dashed line. (b) The relative change of spectra presented in (a). Ratios of broadened absorption spectra relative to that of 0.27 kPa (2 Torr) of CH_2F_2 with no broadening gas in the cell are shown for total pressures of 2.7 kPa (20 Torr: dotted line), 14.7 kPa (110 Torr: short dashed line), and 100 kPa (750 Torr: solid line). The spectrum of 0.27 kPa (2 Torr) of pure CH_2F_2 is shown by the long dashed line.

None of the other hydrohalocarbons studied in the present work exhibited a dependence of IBI on total gas pressure. Thus, it appears that methanes containing heavy Cl, Br atoms can be studied at room temperature without the addition of a broadening gas. The same conclusion can be drawn for the halogenated ethanes studied in the present work as well as for other highly halogenated hydrocarbons that are being considered as CFC alternatives such as C_3 and C_4 haloalkanes, haloethers, etc. This has been confirmed by our investigations of $CH_3CF_2CF_3$ and $CHF_2CH_2CF_3$ in the present work and for hydrofluoroethers [8] as well as by the above-mentioned studies of Roehl et al. [13] and Smith et al. [16].

3.2. Integrated band intensities

Fig. 3 shows the measured absorption spectrum of CH_2F–CF_3 (HFC-134a) as an illustration of the results from this study. The spectra of all compounds studied can be obtained at http://www.nist.gov/kinetics/spectra/index.htm. For the spectral features of interest, IBIs were calculated using the following equation:

$$\mathrm{IBI_{HHC}}(\nu_1 - \nu_2) = \int_{\nu_1}^{\nu_2} \sigma(\nu)\,\mathrm{d}\nu \qquad (2)$$

The units of IBI are cm^2 $molecule^{-1}$ cm^{-1}. The limits of integration are arbitrary to some extent and were chosen to cover the different absorption features and allow the present results to be compared with those available from the literature. Fig. 4 gives an example showing the integrated

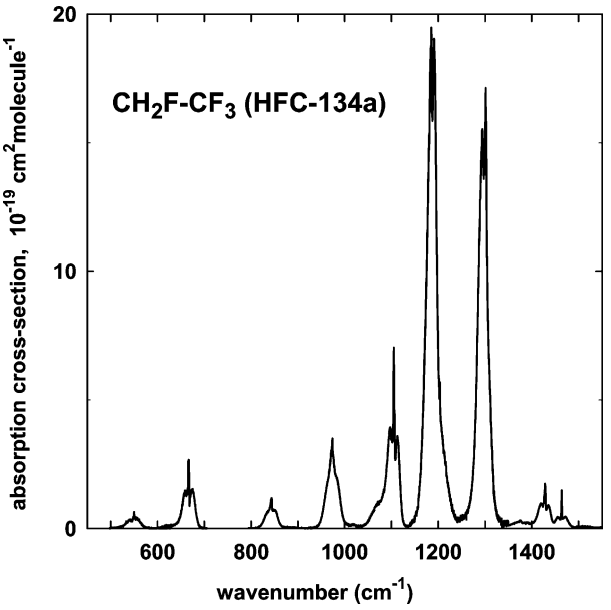

Fig. 3. Absorption cross-sections of $CH_2F–CF_3$ (HFC-134a).

absorbancies over the four strongest bands of CH_2FCF_3 (HFC-134a) versus the sample pressure. The slopes obtained from linear least-square fits of such plots for all compound are the IBIs presented in Tables 1–4.

3.3. Comparison with previous measurements

The available results of IBI measurements at near room temperature are presented in Tables 1–3. $CFCl_3$ is of particular interest as it is used as a reference compound in the estimations of the GWPs of other hydrohalocarbons. The differences between results obtained by various groups are usually larger than the cited individual uncertainties and is probably due to instrumental errors. Nevertheless, a simple averaging of all previous data for the two main absorption bands of $CFCl_3$ (CFC-11) gives values that are in very good agreement with our results (1.1 and 2.1% differences for 800–885 and 1045–1120 cm^{-1}, respectively).

Not all previous papers report intensities for all of the absorption bands of the other halocarbons measured in the present work. Nevertheless, where data are available, we find reasonable agreement between our results and band intensities based on the previous measurements. The IBI obtained here for CF_2Cl_2 (CFC-12) over the 850–950 and 1070–1190 cm^{-1} ranges are 1.3 and 3.9% lower than the averages from the previous studies. IBIs obtained for CHF_2Cl (HCFC-22) are within 1.3% of the average of the previous studies. From Tables 2 and 3 one can see very reasonable agreement between

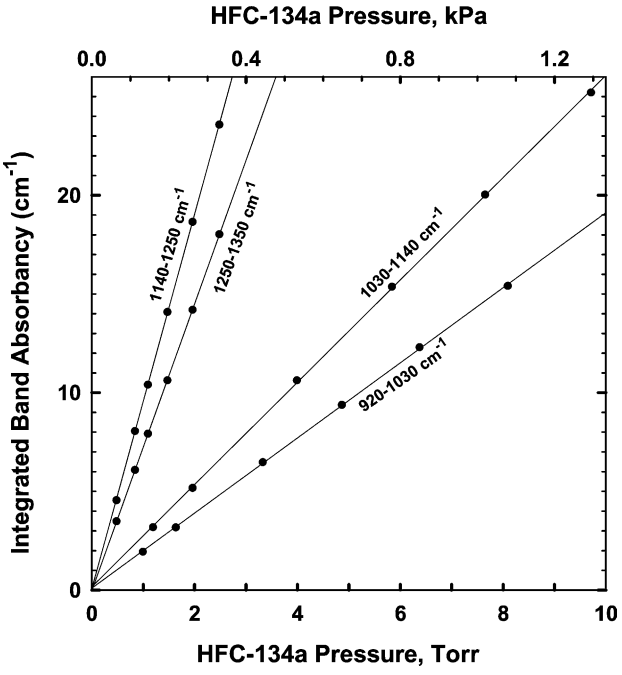

Fig. 4. Measured absorption of the most intensive bands of $CH_2F–CF_3$ (HFC-134a) vs. the HFC-134a pressure in the cell.

Table 1
Integrated room temperature[a] band intensities[b] for $CFCl_3$ (CFC-11)[c]

Integration limits (cm^{-1})[d]			Reference
800–885	910–960	1045–1120	
6.239 ± 0.125		2.920 ± 0.062	[24]
6.98 ± (15%)			[25]
6.279 ± 0.185		2.596 ± 0.145	[26]
6.331 ± 0.177	0.204 ± 0.010	2.401 ± 0.056	[27]
7.312 ± 0.230	0.240 ± 0.010	2.739 ± 0.089	[28]
6.01 ± (10–25%)		2.41 ± (10–25%)	[29]
7.023 ± 0.069		2.743 ± 0.033	[30]
6.866 ± (?)[f]	0.225 ± (?)[f]	2.513 ± (?)	[1][e]
6.534 ± (10%)	0.172 ± (10%)	2.534 ± (10%)	[31]
6.974 ± 0.038		2.591 ± 0.013	[32]
6.461 ± (5%)	0.187 ± (5%)	2.376 ± (5%)	[33]
6.710 ± 0.065	0.220 ± 0.003	2.529 ± 0.012	This work

[a] The data presented were obtained at the temperatures within 293–300 K range.

[b] Units are cm^2 $molecule^{-1}$ cm^{-1}. The uncertainties for the previous works are reported values, whereas the uncertainties in the present work are the 95% confidence intervals and do not include the estimated systematic uncertainty.

[c] Some IBI were presented in units of cm^{-2} atm^{-1} in the original papers. The units were converted into the temperature independent units of cm^2 $molecule^{-1}$ cm^{-1} with the following expression: $\sigma\,(cm^2\,molecule^{-1}\,cm^{-1}) = \sigma\,(cm^{-2}\,atm^{-1}) \times T/n_0/273.15 = \sigma\,(cm^{-2}\,atm^{-1}) \times 1.363 \times 10^{-22} \times T$, where $n_0 = 2.6868 \times 10^{19}$ $molecule\,cm^{-3}$ and T is the temperature indicated in the original paper.

[d] The limits of integration are those used in the present work.

[e] The data obtained by H. Magid (Allied Signal Corp.) were used in [1] for GWP calculations. We used $T = 295$ K to convert to temperature independent units. The original data were obtained at room temperature (Magid, personal communication), while absorption band intensities were probably erroneously reported [1] in units of cm^{-2} atm^{-1} at STP. Uncertainties were not reported.

[f] IBI values for 800–885 and 910–960 cm^{-1} bands were calculated using the reported total IBI over 800–960 cm^{-1} and their ratio obtained in the present study.

Table 2
Integrated band intensities of CFC-12 and HCFC-22

Molecule (compound)	Integration limits (cm^{-1})	IBI (10^{-17} cm^2 $molecule^{-1}$ cm^{-1})											
		[34]	[26]	[28]	[29]	[35]	[30]	[1][a]	[31]	[36]	[37]	[19]	This work
CF_2Cl_2 (CFC-12)	850–900		5.322	1.150	6.131	6.123	5.809	5.722	1.101		5.880		1.227 ± 0.023
	900–950			4.683					4.354				4.480 ± 0.054
	1070–1130		4.644	4.602	7.139	8.060	4.615	7.117	4.206		4.497		4.353 ± 0.061
	1130–1190		2.935	3.134			2.931		2.925		3.083		2.853 ± 0.051
CHF_2Cl (HCFC-22)	750–860						2.233	2.276	2.132	2.335	2.357	10.1	2.260 ± 0.011
	1050–1200						7.179	6.722	6.007	6.863	6.825		6.631 ± 0.045
	1280–1380							1.265	0.882	1.066	1.081		1.079 ± 0.009
CF_3Br (H-1301)	720–790	0.488											0.545 ± 0.022
	1040–1150	7.698					8.074						7.973 ± 0.162
	1150–1250	7.718					7.918						7.833 ± 0.156

Some IBI were presented in units of cm^{-2} atm^{-1} in the original papers. The units were converted into the temperature independent units of cm^2 $molecule^{-1}$ cm^{-1} with the following expression: σ (cm^2 $molecule^{-1}$ cm^{-1}) = σ (cm^{-2} atm^{-1}) × $T/n_0/273.15$ = σ (cm^{-2} atm^{-1}) × 1.363 × 10^{-22} × T, where $n_0 = 2.6868 \times 10^{19}$ molecule cm^{-3} and T is the temperature indicated in the original paper.

[a] See footnote e for Table 1.

results of the present study and the results from previous measurements for Halon-1301, HCFC-123, HFC-125, HFC-134a, HCFC-141b, and HFC-32 (see Table 3). Brown et al. [18] also report IBIs for HCFC-123, HFC-125, HFC-134a, HCFC-141b, and H-1311. However, for these determinations, they only evaluated the wavelength interval between 800 and 1200 cm^{-1}. Hence, we cannot compare their results with those reported in this work since contributions from absorption features outside of this interval are significant.

Some comments bear mentioning about the CH_2F_2 (HFC-32) data. There is an excellent coincidence with the results obtained by Smith et al. [16] using undiluted samples (presented in Table 3). These authors measured spectra with higher resolution (0.03 cm^{-1} versus 0.5 cm^{-1} in our experiments). At our 0.5 cm^{-1} spectral resolution we had a band intensity underestimation of approximately 40% in the experiments with no broadening gas added (see Section 3.1 and Fig. 1). Such underestimation should have been negligible at the 17 times better instrumental resolution used by Smith et al. [16]. The original total band intensity of CH_2F_2 reported by Pinnock et al. [19] was ca. 8% higher than measured here. However, these authors now believe that their value was 8% too high (Hurley, personal communication reported in [20]). Thus, the HFC-32 band intensities can be considered as well established.

4. Global warming potentials and radiative forcing

The GWP has been introduced as a simple index for comparing different greenhouse gases. It is defined [2] as the time-integrated radiative forcing, due to the instantaneous release of a chemical into the atmosphere, expressed relative to that of the same mass of CO_2:

$$\mathrm{GWP}(t) = \frac{\int_0^t a_i c_i(t)/M_i \,\mathrm{d}t}{\int_0^t a_{\mathrm{CO_2}} c_{\mathrm{CO_2}}(t)/M_{\mathrm{CO_2}} \,\mathrm{d}t} \tag{3}$$

where a_i is the radiative forcing due to a unit increase in the molar concentration, $c_i(t)$ of trace gas, i; remaining at time, t, after its release over which the calculation is performed.

Being a relative parameter, it can be calculated more accurately than the absolute change due to emission of a single substance. There are two reasons for considering different time horizons in the calculation of GWP. For some environmental feedbacks it is important to evaluate both the relatively short and long-term effects due to release of greenhouse gases. Secondly, the degradation process of CO_2 on a global scale is complicated by exchange among different reservoirs and, therefore, cannot be described correctly by a single atmospheric lifetime.

Fisher et al. [1] introduced the halocarbon global warming potential (HGWP) as the ratio of the calculated steady state infrared radiative forcing due to the steady state emission of a compound into the atmosphere to that of CFC-11:

$$\mathrm{HGWP} = \frac{(\text{calculated radiative forcing due to steady state emission of compound, } i)/W_i}{(\text{calculated radiative forcing due to steady state emission of CFC-11})/W_{\mathrm{CFC\text{-}11}}}$$

where W_i is the emission rate (mass emission) of the compound i. The above expression can be rewritten as

$$\mathrm{HGWP} = \frac{a_i c_i/W_i}{a_{\mathrm{CFC\text{-}11}} c_{\mathrm{CFC\text{-}11}}/W_{\mathrm{CFC\text{-}11}}} = \frac{a_i \tau_i/M_i}{a_{\mathrm{CFC\text{-}11}} \tau_{\mathrm{CFC\text{-}11}}/M_{\mathrm{CFC\text{-}11}}} \tag{4}$$

Table 3
Integrated band intensities of HFC-32, HCFC-123, HFC-125, HFC-134a, HCFC-141b, and methyl chloroform

Molecule (compound)	Integration limits (cm^{-1})	IBI (10^{-17} cm^2 $molecule^{-1}$ cm^{-1})							
		[1][a]	[36]	[37]	[38]	[19]	[15]	[16]	This work
CH_2F_2 (HFC-32)	450–600								0.079 ± 0.004
	1020–1220					6.3[b]		5.68[c]	5.67 ± 0.17
	1380–1480					(5.83)[b]		0.168[c]	0.164 ± 0.003
$CHCl_2$–CF_3 (HCFC-123)	480–535				0.0645				0.074 ± 0.002
	535–590				0.0500				0.063 ± 0.002
	590–644				0.0386				0.037 ± 0.002
	644–700	0.450	0.431		0.388	12.8			0.402 ± 0.012
	700–800	2.320	2.228	2.39	0.289				0.294 ± 0.004
	800–855				1.988				1.618 ± 0.026
	855–900								0.382 ± 0.006
	960–1040				0.152				0.102 ± 0.003
	1040–1090				0.122				0.085 ± 0.002
	1090–1170	8.727	10.087	10.49	2.854				2.718 ± 0.081
	1170–1255				3.404				3.509 ± 0.105
	1255–1305				2.247				2.422 ± 0.072
	1305–1430				1.125				1.375 ± 0.041
CHF_2–CF_3 (HFC-125)	460–550	0.406			0.102				0.117 ± 0.004
	550–610				0.223				0.230 ± 0.009
	680–760	1.141		0.53	0.516	16.1			0.563 ± 0.022
	810–920			0.67	0.674				0.726 ± 0.036
	1060–1170	14.166		14.91	3.908				3.948 ± 0.020
	1170–1270				10.362				8.289 ± 0.041
	1270–1335								2.468 ± 0.012
	1335–1375				0.150				0.112 ± 0.033
	1375–1412								0.056 ± 0.002
	1412–1480				0.059				0.082 ± 0.002
CH_2F–CF_3 (HFC-134a)	490–600				0.156				0.148 ± 0.002
	600–700	0.559	0.539		0.532	13.1	0.560		0.512 ± 0.005
	800–920	0.338	0.236	0.25	0.251		0.2429		0.272 ± 0.004
	920–1030	12.260	0.850	0.79	0.887		0.8525		0.916 ± 0.012
	1030–1140		1.417	1.41	1.492		1.486		1.492 ± 0.018
	1140–1250		9.649	9.71	5.509				5.469 ± 0.033
	1250–1350				4.154		9.881		4.171 ± 0.021
	1350–1395		0.463	0.45					0.098 ± 0.002
	1395–1448				0.322		0.4812		0.330 ± 0.006
	1448–1510				0.138				0.154 ± 0.003
	1510–1550								0.018 ± 0.001
CH_3–CCl_2F (HCFC-141b)	540–630	0.330			0.319				0.335 ± 0.005
	670–800	7.064		2.37	2.238	7.8			2.330 ± 0.019
	800–860								0.045 ± 0.001
	880–980			1.09	1.045				1.085 ± 0.022
	980–1030								0.056 ± 0.001
	1030–1138			3.95	2.319				2.371 ± 0.033
	1138–1220				1.355				1.395 ± 0.019
	1350–1420	0.294		0.34	0.265				0.269 ± 0.003
	1420–1480				0.075				0.080 ± 0.001
	1480–1540								0.022 ± 0.001
CH_3–CCl_3	480–570								0.124 ± 0.005
	650–775	2.889							3.037 ± 0.020
	775–890								0.049 ± 0.003
	975–1030	1.681							0.043 ± 0.001
	1030–1140								1.605 ± 0.048
	1215–1270								0.023 ± 0.001
	1350–1405	0.129							0.122 ± 0.004
	1405–1490								0.134 ± 0.005

[a] See footnote e for Table 1.

[b] Pinnock et al. [19] reported the total IBI measured over the 700–1600 cm^{-1} range to be 6.3×10^{-17} cm^2 $molecule^{-1}$ cm^{-1} at $T = 296$ K. Authors believe now that the value is 8% too high (personal communication, 1998, reported in [20]). Therefore, their corrected value is 5.83×10^{-17} cm^2 $molecule^{-1}$ cm^{-1} (compared to our value of 5.834×10^{-17} cm^2 $molecule^{-1}$ cm^{-1}).

[c] The presented values were obtained from the measurements in pure CH_2F_2 sample (100–150 Pa) with 0.03 cm^{-1} spectral resolution. Pressurizing the sample with dry air (up to 100 kPa) resulted in the decrease of the measured band intensities that is probably an experimental artifact.

Table 4
Integrated band intensities of HCFC-122, HCFC-122a, HCFC-123a, HFC-132c, H-1201, H-2301, H-2311, and H-2401

Molecule (compound)	Integration limits (cm^{-1})	IBI (10^{-17} cm^2 $molecule^{-1}$ cm^{-1})
$CHCl_2$–CF_2Cl (HCFC-122)	560–610	0.276 ± 0.008
	610–660	0.105 ± 0.003
	720–790	1.227 ± 0.006
	790–890	1.623 ± 0.008
	890–946	0.051 ± 0.002
	946–1010	1.368 ± 0.041
	1010–1095	1.443 ± 0.043
	1095–1175	2.683 ± 0.081
	1175–1250	1.183 ± 0.036
	1250–1316	0.444 ± 0.013
	1316–1360	0.027 ± 0.001
CHFCl–$CFCl_2$ (HCFC-122a)	590–670	0.650 ± 0.017
	710–768	0.411 ± 0.002
	768–828	1.655 ± 0.008
	828–860	0.520 ± 0.003
	860–940	2.142 ± 0.011
	940–1010	0.345 ± 0.005
	1010–1075	1.029 ± 0.016
	1075–1128	1.902 ± 0.030
	1128–1158	0.546 ± 0.009
	1158–1230	0.413 ± 0.006
	1230–1300	0.224 ± 0.005
	1300–1380	0.181 ± 0.004
CHFCl–CF_2Cl (HCFC-123a)	450–520	0.039 ± 0.002
	570–690	0.634 ± 0.019
	740–823	1.426 ± 0.014
	823–910	1.071 ± 0.011
	930–1025	1.585 ± 0.032
	1025–1082	1.296 ± 0.026
	1082–1124	1.678 ± 0.033
	1124–1205	3.552 ± 0.071
	1205–1310	1.212 ± 0.024
	1210–1400	0.263 ± 0.003
CH_2F–$CFCl_2$ (HCFC-132c)	425–485	0.071 ± 0.003
	550–605	0.113 ± 0.003
	605–680	0.695 ± 0.021
	710–800	0.418 ± 0.012
	800–895	2.229 ± 0.029
	895–964	1.269 ± 0.016
	964–1020	0.079 ± 0.002
	1020–1085	0.969 ± 0.019
	1085–1142	1.041 ± 0.021
	1142–1220	1.071 ± 0.021
	1220–1340	0.379 ± 0.007
	1340–1415	0.065 ± 0.002
	1415–1490	0.085 ± 0.002
CH_3–CF_2–CF_3 (HFC-245cb)[a]	472–542	0.175 ± 0.010
	614–680	0.526 ± 0.020
	756–790	0.050 ± 0.003
	908–946	0.359 ± 0.015
	946–1050	0.500 ± 0.020
	1065–1163	2.822 ± 0.060
	1163–1266	12.44 ± 0.250
	1266–1322	0.136 ± 0.004
	1322–1433	0.940 ± 0.030
	1433–1490	0.149 ± 0.005
CHF_2–CH_2–CF_3 (HFC-245fa)	455–515	0.196 ± 0.020
	515–620	0.276 ± 0.014
	650–710	0.364 ± 0.015
	820–870	0.283 ± 0.010
	870–945	0.476 ± 0.015
	950–1036	0.159 ± 0.006
	1036–1099	2.307 ± 0.050
	1099–1144	1.471 ± 0.040
	1144–1224	7.335 ± 0.150
	1224–1275	1.832 ± 0.045
	1275–1320	1.702 ± 0.045
	1320–1360	0.859 ± 0.025
	1360–1398	0.657 ± 0.020
	1398–1485	1.915 ± 0.055
CHF_2Br (Halon-1201)[b]	530–610	0.083 ± 0.002
	610–670	0.031 ± 0.001
	670–750	1.728 ± 0.011
	830–920	0.049 ± 0.001
	990–1050	0.118 ± 0.004
	1050–1190	6.722 ± 0.134
	1240–1310	1.189 ± 0.009
	1310–1400	0.138 ± 0.002
CH_2Br–CF_3 (Halon-2301)	590–670	0.394 ± 0.002
	670–780	0.322 ± 0.004
	800–900	0.193 ± 0.001
	1036–1110	1.444 ± 0.019
	1110–1190	3.837 ± 0.046
	1190–1261	1.316 ± 0.013
	1261–1298	2.419 ± 0.024
	1298–1340	1.864 ± 0.019
	1340–1460	0.489 ± 0.003
	1460–1510	0.080 ± 0.001
CHClBr–CF_3 (Halon-2311)	480–530	0.075 ± 0.003
	530–570	0.069 ± 0.002
	630–685	0.400 ± 0.017
	685–740	0.344 ± 0.005
	770–840	1.190 ± 0.008
	840–895	0.370 ± 0.007
	895–940	0.023 ± 0.001
	1090–1157	2.582 ± 0.051
	1157–1247	3.605 ± 0.072
	1247–1295	2.804 ± 0.056
	1295–1370	1.549 ± 0.031
CHFBr–CF_3 (Halon-2401)	490–540	0.099 ± 0.003
	540–580	0.083 ± 0.003
	670–710	0.806 ± 0.017
	710–810	0.539 ± 0.011
	810–895	0.633 ± 0.022
	1030–1125	1.856 ± 0.024
	1125–1180	3.220 ± 0.042
	1180–1240	3.598 ± 0.047
	1240–1334	2.785 ± 0.036
	1334–1410	0.883 ± 0.008
	1410–1480	0.066 ± 0.002

[a] Christidis et al. [33] reported the total IBI measured over the 450–2000 cm^{-1} range to be 15.77×10^{-17} cm^2 $molecule^{-1}$ cm^{-1} at $T = 296$ K (compared to our value of 18.1×10^{-17} cm^2 $molecule^{-1}$ cm^{-1}).

[b] Christidis et al. [33] reported the total IBI measured over the 450–2000 cm^{-1} range to be 9.91×10^{-17} cm^2 $molecule^{-1}$ cm^{-1} at $T = 296$ K (compared to our value of 10.06×10^{-17} cm^2 $molecule^{-1}$ cm^{-1}).

where c_i is the atmospheric concentration of trace gas, i; M_i and τ_i are its molecular mass and the residence time in the atmosphere, respectively.

Unlike the GWP as discussed above, the definition of HGWP is not inherently time dependent. However, a simple extension of the definition will allow for time horizons. One can consider a compound to be characterized by a single decay time, τ_i (an atmospheric lifetime in the case of CFCs, HFCs and HCFCs). In the case of emission into the atmosphere at a steady state rate, W_i, the molar concentration is described as

$$c_i(t) \sim W_i \tau_i \frac{1 - \exp(-t/\tau_i)}{M_i} \tag{5}$$

Hence, a time dependent value, HGWP(t) can be introduced for the case of steady state emission of a compound into the atmosphere, by analogy with HGWP:

$$\mathrm{HGWP}(t) = \frac{a_i}{a_{\mathrm{CFC\text{-}11}}} \frac{M_{\mathrm{CFC\text{-}11}}}{M_i} \frac{\tau_i}{\tau_{\mathrm{CFC\text{-}11}}} \frac{1-\exp(-t/\tau_i)}{1-\exp(-t/\tau_{\mathrm{CFC\text{-}11}})} \tag{6}$$

and HGWP is simply HGWP ($t \to \infty$).

On the other hand, in the case of the instantaneous release of mass ϑ of the compound into the atmosphere

$$c_i(t) \sim \frac{\vartheta \exp(-t/\tau_i)}{M_i} \tag{7}$$

and one can derive by analogy with Eq. (3)

$$\mathrm{HGWP}(t) = \frac{\int_0^t a_i c_i(t)/M_i \, \mathrm{d}t}{\int_0^t a_{\mathrm{CFC\text{-}11}} c_{\mathrm{CFC\text{-}11}}(t)/M_{\mathrm{CFC\text{-}11}} \, \mathrm{d}t} = \frac{a_i}{a_{\mathrm{CFC\text{-}11}}} \frac{M_{\mathrm{CFC\text{-}11}}}{M_i} \frac{\tau_i}{\tau_{\mathrm{CFC\text{-}11}}} \frac{1 - \exp(-t/\tau_i)}{1 - \exp(-t/\tau_{\mathrm{CFC\text{-}11}})} \tag{8}$$

Thus, from the kinetic point of view, HGWP(t) and GWP(t) are essentially the same, except different reference gases are used.

In general, to calculate the value of a GWP one should integrate the absorption of IR radiation over time, altitude, and wavenumber

$$\mathrm{GWP}_i(t) = \frac{\int_0^t \int_0^h \int_{\nu_1}^{\nu_2} c_i(h,t)\sigma_i(\nu)\Phi(\nu,h) \, \mathrm{d}\nu \, \mathrm{d}h \, \mathrm{d}t}{\int_0^t \int_0^h \int_{\nu_1}^{\nu_2} c_{\mathrm{ref}}(h,t)\sigma_{\mathrm{ref}}(\nu)\Phi(\nu,h) \, \mathrm{d}\nu \, \mathrm{d}h \, \mathrm{d}t} \tag{9}$$

where $\sigma_i(\nu)$ is the absorption cross-section of the compound, i; h the altitude, and $\Phi(\nu, h)$ is the flux of the Earth's outgoing radiation. However, even a simple consideration shows that the absorption of the Earth's outgoing radiation by a well-mixed greenhouse gas takes place mainly in the troposphere and tropopause regions. Fig. 5 shows results of our rudimentary calculations to illustrate the integrated absorption of the Earth's radiation by an IR active gas. The Earth's surface temperature was accepted to be $T = 288\,\mathrm{K}$ and absorption by the two-level modeled gas being in thermal equilibrium in the atmosphere was calculated. The altitudinal temperature profile (shown in Fig. 5) and the barometric gas density distribution govern the absorption of the outgoing radiation. The upper sheaf of lines show the cumulative absorption (i.e. integrated from the surface to a particular altitude) at 600, 1000, and 1400 cm^{-1}, respectively, by a gas whose mixing ratio is constant up to 50 km. The lower sheaf of lines show the results of analogous calculations for a compound with a fast stratospheric sink such as $CFCl_3$, CFC-11 (whose mixing ratio is shown in Fig. 5). Fig. 5 shows that even in the case of a compound with a fast stratospheric sink (which results in a decreasing mixing ratio at higher altitudes) ca. 90% of the total absorption takes place in the altitude region where the chemical is still uniformly distributed. The results of field measurements as well as model calculations show that hydrohalocarbon volume mixing ratios are fairly constant over that region of the atmosphere even for compounds with relatively fast stratospheric sinks, like $CFCl_3$ (CFC-11). This allows one to simplify calculations by using average atmospheric mixing ratios of compounds rather than integrating their vertical profiles.

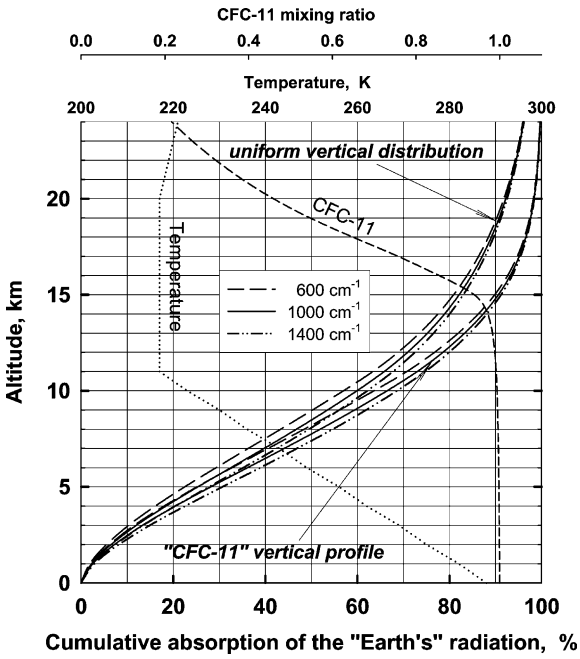

Fig. 5. Calculated cumulative absorption of the outgoing surface radiation by a modeled two-level absorbing gas in the atmosphere at 600, 1000, and 1400 cm^{-1}. The upper sheaf of lines illustrates results obtained for a gas with a constant mixing ratio from the surface up to 50 km. The lower one illustrates those for a gas whose mixing ratio is similar to that of CFC-11 (dashed line). The altitudinal temperature profile is shown by the dotted line.

The lifetimes of well-mixed hydrogen-containing compounds can be calculated based on the rate constants for their reactions with OH and the OH-driven lifetime of methyl chloroform [5]:

$$\tau_i^{\mathrm{OH}} = \frac{k_{\mathrm{MC}}(272)}{k_i(272)} \tau_{\mathrm{MC}}^{\mathrm{OH}} \tag{10}$$

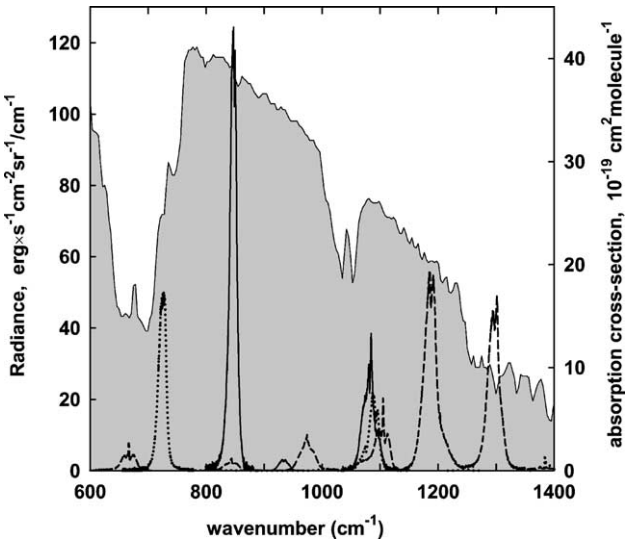

Fig. 6. The measured spectrum of the Earth's outgoing radiation obtained by NIMBUS 4 [23] (shaded area) and the absorption spectra of some halogenated alkanes: $CFCl_3$ (solid line), CH_3CCl_3 (dotted line), and CH_2FCF_3 (dashed line).

where τ_i^{OH} and $\tau_{MC}^{OH} = 5.9$ years are the atmospheric lifetimes of the compound under study and MC, respectively, due to reactions with hydroxyl radicals in the troposphere only, and $k_i(272)$ and $k_{MC}(272) = 6.0 \times 10^{-15}$ cm^3 molecule^{-1} s^{-1} [21] are the rate constants for the reactions of OH with these substances at $T = 272$ K. The value of $\tau_{MC}^{OH} = 5.9$ years was obtained from the measured lifetime of MC, $\tau_{MC} = 4.8$ years [3] when ocean loss, 85 years [22] and stratospheric loss, 38 years are taken into account.

In order to develop a similar simple technique for the estimation of radiative forcing, we assume a uniform vertical distribution of radiative flux and disregard absorption by other greenhouse gases in the atmosphere. Fig. 6 illustrates the validity of this assumption. It is certainly not correct in the region of the 15 μm (667 cm^{-1}) absorption band of CO_2. To a lesser extent, this assumption can also cause an error for compounds that have their main absorption bands in the region of the 9.6 μm (1040 cm^{-1}) ozone band and of water absorption below 8.3 μm (above 1200 cm^{-1}). Nevertheless, the simplicity of such an estimation is very attractive. This estimation procedure is similar to that of Pinnock et al. [19] who suggested the use of a model calculated irradiance at the tropopause for estimating the GWPs of radiatively important atmospheric gases.

We have calculated the relative radiative forcings (using CFC-11 as a reference), $RRF_i^{CFC\text{-}11}$ for all of the halocarbons of this study in order to compare them with the results from available radiative transfer models:

$$RRF_i^{CFC\text{-}11} = \frac{a_i}{a_{CFC\text{-}11}} = \frac{\int_{\nu_1}^{\nu_2} \sigma_i(\nu)\Phi(\nu)\,d\nu}{\int_{\nu_1}^{\nu_2} \sigma_{CFC\text{-}11}(\nu)\Phi(\nu)\,d\nu} \quad (11)$$

where $\Phi(\nu)$ is the intensity of outgoing Earth's radiation, ν_1 and ν_2 are the integration limits (450 and 1600 cm^{-1}, respectively, in our calculations). We used the experimentally measured spectrum of outgoing Earth's radiation obtained from the NIMBUS-4 satellite at a latitude of 15°N [23] in these calculations. The results are presented in Table 5. The values for HGWP and HGWP(t) were then calculated using Eqs. (4) and (8), and are presented in Table 6. Table 5 also gives radiative forcing values obtained from atmospheric model calculations. We decided to compare the calculated radiative forcing, not the GWP, because these intermediate parameters are not affected by the values used for the atmospheric lifetimes. Table 5 shows that our simple calculations provide very reasonable estimates of radiative forcing. The only serious disagreement was obtained in the case of methyl chloroform, whose main absorption band overlaps the 15 μm absorption band of CO_2 (see Fig. 6).

All the atmospheric parameters discussed above τ_i, $RRF_i^{CFC\text{-}11}$, and $HGWP_i(t)$ are the results of self-consistent estimations made using only data from laboratory measurements (k_i, $\sigma_i(\nu)$) and field measurements (τ_{MC}, $\Phi(\nu)$). GWPs with CO_2 as a reference (GWP_i) cannot be

Table 5
Radiative forcing of selected hydrohaloalkanes relative to that of CFC-11

Compound	Molecule	This work	[1]	[37]	[19]	[39]	[40]	[33]	[20]
CFC-11	$CFCl_3$	1.0	1.0	1.0	1.0	1.0	1.0	1.0	1.0
CFC-12	CF_2Cl_2	1.15	1.23; 1.50			1.27	1.28		1.28
HCFC-22	CHF_2Cl	0.79	0.84; 0.91	0.85	0.84	0.86	0.71		0.88
HFC-32	CH_2F_2	0.44			0.51[a]	0.50[a]			0.52[a]
HCFC-123	$CHCl_2$–CF_3	0.83	0.71; 0.83	0.90	0.76	0.82			0.80
HFC-125	CHF_2–CF_3	0.98	0.95; 1.21	0.91	0.92	0.91			0.92
HFC-134a	CH_2F–CF_3	0.74	0.72; 0.83	0.78	0.66	0.77			0.76
HCFC-141b	CH_3–$CFCl_2$	0.68	0.57; 0.64	0.66	0.59	0.64			0.56
MC	CH_3–CCl_3	0.38	0.24; 0.20			0.23			0.24
HFC-245cb	CH_3–CF_2–CF_3	1.08						0.96	1.04
H-1201	CHF_2Br	0.68						0.63	0.56
H-1301	CF_3Br	1.14				1.27			1.28

[a] An estimation based on the IR spectrum measured by Pinnock et al. [19]. Authors believe now that it is 8% too high (personal communication, 1998, reported in [20]). Therefore, the corrected value should be 0.46–0.48.

Table 6
Relative radiative forcing, atmospheric lifetime, and GWPs of some halogenated alkanes

Compound	Molecule	Atmospheric lifetime (years)	$RRF_i^{CFC\text{-}11}$	HGWP	HGWP (GWP) at time horizons (years)		
					20	100	500
CFC-11	$CFCl_3$	50.0[a]	1.00	1.0	1.0 (5000)	1.0 (4000)	1.0 (1400)
CFC-12	CF_2Cl_2	102.0[a]	1.15	2.66	1.44 (7200)	1.9 (7700)	2.6 (3700)
HCFC-22	CHF_2Cl	12.2	0.79	0.30	0.74 (3700)	0.35 (1400)	0.30 (430)
HFC-32	CH_2F_2	5.4	0.44	0.12	0.37 (1800)	0.14 (580)	0.12 (170)
HCFC-122	$CHCl_2$–CF_2Cl	0.97	0.88	0.014	0.042 (210)	0.016 (64)	0.014 (20)
HCFC-122a	CHFCl–$CFCl_2$	3.4	0.91	0.051	0.15 (770)	0.059 (240)	0.051 (71)
HCFC-123	$CHCl_2$–CF_3	1.4	0.83	0.021	0.063 (310)	0.024 (96)	0.021 (29)
HCFC-123a	CHFCl–CF_2Cl	4.2	0.98	0.073	0.22 (1100)	0.085 (340)	0.073 (100)
HFC-125	CHF_2–CF_3	31.0	0.98	0.70	1.0 (5000)	0.78 (3100)	0.70 (980)
HCFC-132c	CH_2F–$CFCl_2$	4.3	0.74	0.064	0.19 (960)	0.074 (290)	0.064 (89)
HFC-134a	CH_2F–CF_3	14.0	0.74	0.28	0.64 (3200)	0.32 (1300)	0.28 (390)
HCFC-141b	CH_3–$CFCl_2$	10.3	0.68	0.16	0.43 (2100)	0.19 (760)	0.16 (230)
HFC-245fa	CHF_2–CH_2–CF_3	7.5	1.11	0.17	0.48 (2400)	0.20 (800)	0.17 (240)
HFC-245cb	CH_3–CF_2–CF_3	38.0	1.08	0.85	1.04 (5200)	0.91 (3600)	0.85 (1200)
H-1301	CF_3Br	65.0[a]	1.14	1.37	1.1 (5500)	1.25 (5000)	1.37 (1900)
H-1201	CHF_2Br	5.4	0.68	0.076	0.23 (1100)	0.088 (350)	0.076 (110)
H-1202	CF_2Br_2	3.9[a]	1.13	0.058	0.17 (870)	0.067 (270)	0.058 (80)
H-2301	CH_2Br–CF_3	3.4	0.67	0.038	0.12 (580)	0.044 (180)	0.038 (54)
H-2311	$CHClBr$–CF_3	1.0	0.79	0.012	0.035 (170)	0.013 (53)	0.011 (16)
H-2401	$CHFBr$–CF_3	2.9	0.87	0.030	0.089 (450)	0.034 (140)	0.030 (41)

[a] The atmospheric lifetime is taken from [39].

accurately calculated in the above-described manner due to the high concentration of carbon dioxide in the real Earth's atmosphere, which results in non-linear absorption of the Earth's outgoing radiation by CO_2 molecules. Therefore, we have used the GWP of CFC-11 referenced to CO_2 ($GWP_{CFC\text{-}11}$) calculated using a radiative transfer model of the atmosphere and accepted in the 1998 International Scientific Assessment of Ozone Depletion [20] to obtain GWPs:

$$GWP_i(t) = HGWP_i(t) \times GWP_{CFC\text{-}11}(t) \quad (12)$$

This estimation procedure is not valid for gases with very short atmospheric lifetimes, since they do not have a uniform mixing ratio either vertically in the upper troposphere and tropopause region or geographically with latitude as does the CFC-11 reference compound.

5. Conclusions

The infrared absorption spectra of 21 halogenated alkanes were measured in the spectral range 400 and 1600 cm^{-1}. An analysis of the effects of added inert gas shows that IR absorption band intensities of deeply halogenated alkanes in the range of atmospheric transparency window can usually be determined even without pressure broadening with moderate spectral resolution. Direct GWPs were determined using these measured spectra and a simple numerical procedure based on the measured spectrum of the Earth's outgoing radiation. The results obtained with this procedure agree with those from elaborate modeling calculations.

Acknowledgements

We would like to thank Dr. Pamela Chu (NIST) for her help in measuring the IR spectra using the FTIR spectrophotometer. The work done in the Institute of Energy Problems of Chemical Physics was supported by the Russian Basic Research Foundation, Grant 93-03-112358.

References

[1] D.A. Fisher, C.H. Hales, W.-C. Wang, M.K.W. Ko, N.D. Sze, Nature 344 (1990) 513–516.
[2] J.T. Houghton, G.J. Jenkins, J.J. Ephraums (Eds.), Climate Change: The IPCC Scientific Assessment, Intergovernmental Panel on Climate Change (IPCC), Cambridge University Press, Cambridge, UK, 1990.
[3] R.G. Prinn, R.F. Weiss, B.R. Miller, J. Huang, F.N. Alyea, D.M. Cunnold, P.J. Fraser, D.E. Hartley, P.G. Simmonds, Science 269 (1995) 187–192.
[4] M. Prather, C.M. Spivakovsky, J. Geophys. Res. 95 (1990) 18723–18729.
[5] C.M. Spivakovsky, J.A. Logan, S.A. Montzka, Y.J. Balkanski, M. Foreman-Fowler, D.B.A. Jones, L.W. Horowitz, A.C. Fusco, C.A.M. Brenninkmeijer, M.J. Prather, S.C. Wofsy, M.B. McElroy, J. Geophys. Res. 105 (2000) 8931–8980.
[6] V.L. Orkin, V.G. Khamaganov, A.G. Guschin, E.E. Kasimovskaya, I.K. Larin, Development of atmospheric characteristics of chlorine-free alternative fluorocarbons, Report on R-134a and E-143a, Report ORNL/Sub/86X-SL103V prepared for the Oak Ridge National Laboratory, 1993.
[7] V.L. Orkin, V.G. Khamaganov, A.G. Guschin, R.E. Huie, M.J. Kurylo, in: Proceedings of the 13th International Symposium on Gas Kinetics, The University College of Dublin, Dublin, Ireland, 1994, pp. 359–360.
[8] V.L. Orkin, E. Villenave, R.E. Huie, M.J. Kurylo, J. Phys. Chem. 103 (1999) 9770–9779.

[9] A.G. Guschin, E.E. Kasimovskaya, I.K. Larin, V.L. Orkin, V.G. Khamaganov, Zhurnal Organicheskoi Khimii 30 (1994) 1156–1162.
[10] V.L. Orkin, R.E. Huie, M.J. Kurylo, J. Phys. Chem. 101 (1997) 9118–9124.
[11] E.B. Wilson Jr., A.J. Wells, J. Chem. Phys. 14 (1946) 578–580.
[12] S.S. Penner, D. Weber, J. Chem. Phys. 19 (1951) 807–817.
[13] C.M. Roehl, D. Boglu, C. Bròhl, G.K. Moorgat, Geophys. Res. Lett. 22 (1995) 815–818.
[14] D. Newnham, J. Ballard, J. Quant. Spectrosc. Radiat. Trans. 53 (1995) 471–479.
[15] D. Newnham, J. Ballard, M. Page, J. Quant. Spectrosc. Radiat. Trans. 55 (1996) 373–381.
[16] K. Smith, D. Newnham, M. Page, J. Ballard, G. Duxbury, J. Quant. Spectrosc. Radiat. Trans. 56 (1996) 73–82.
[17] K. Smith, D. Newnham, M. Page, J. Ballard, G. Duxbury, J. Quant. Spectrosc. Radiat. Trans. 59 (1998) 437–451.
[18] A.C. Brown, C.E. Canosa-Mas, A.D. Parr, R.P. Wayne, Atmos. Environ. 24A (1990) 2499–2511.
[19] S. Pinnock, M.D. Hurley, K.P. Shine, T.J. Wallington, T.J. Smyth, J. Geophys. Res. 100 (1995) 23227–23238.
[20] World Meteorological Organization, Scientific Assessment of Ozone Depletion: 1998, Global Ozone Research and Monitoring Project, Report No. 44, 1999.
[21] S.P. Sander, R.R. Friedl, D.M. Golden, M.J. Kurylo, R.E. Huie, V.L. Orkin, G.K. Moortgat, A.R. Ravishankara, C.E. Kolb, M.J. Molina, B.J. Finlayson-Pitts, Chemical kinetics and photochemical data for use in atmospheric studies, Evaluation No. 14 of the NASA Panel Data Evaluation, JPL Publication 02-25; Jet Propulsion Laboratory, California Institute of Technology, Pasadena, CA, 1 February 2003.
[22] J.H. Butler, J.W. Elkins, T.M. Thompson, B.D. Ball, T.H. Swanson, V. Koropalov, J. Geophys. Res. 96 (1991) 22347–22355.
[23] V.G. Kunde, B.J. Conrath, R.A. Hanel, W.C. Maguire, C. Prabhakara, V.V. Salomonson, J. Geophys. Res. 79 (1974) 777–784.
[24] J. Herranz, R. de la Cierva, J. Morcillo, Ann. Real Soc. Espan. Fis. Quim. A55 (1959) 69–76.
[25] A. Goldman, F.S. Bonomo, D.G. Murcray, Appl. Optics 15 (1976) 2305–2307.
[26] P. Varanasi, F.K. Ko, J. Quant. Spectrosc. Radiat. Trans. 17 (1977) 385–388.
[27] R. Nanes, P.M. Silvaggio, R.W. Boese, J. Quant. Spectrosc. Radiat. Trans. 23 (1980) 211–220.
[28] R.H. Kagann, J.W. Elkins, R.L. Sams, J. Geophys. Res. 88 (1983) 1427–1432.
[29] S.T. Massie, A. Goldman, D.G. Murcray, J.C. Gille, Appl. Optics 24 (1985) 3426–3427.
[30] P. Varanasi, S. Chudamani, J. Geophys. Res. 93 (1988) 1666–1668.
[31] A.H. McDaniel, C.A. Cantrell, J.A. Davidson, R.E. Shetter, J.G. Calvert, J. Atmos. Chem. 12 (1991) 211–227.
[32] Z. Li, P. Varanasi, J. Quant. Spectrosc. Radiat. Trans. 52 (1994) 137–144.
[33] N. Christidis, M.D. Hurley, S. Pinnock, K.P. Shine, T.J. Wallington, J. Geophys. Res. 102 (1997) 19597–19609.
[34] W.B. Person, S.R. Polo, Spectrochim. Acta 17 (1961) 101–111.
[35] N. Van-Thanh, I. Rossi, A. Jean-Louis, H. Rippel, J. Geophys. Res. 91 (1986) 4056–4062.
[36] F. Cappellani, G. Restelli, Spectrochim. Acta 48A (1992) 1127–1131.
[37] C. Clerbaux, R. Colin, P.C. Simon, C. Granier, J. Geophys. Res. 98 (1993) 10491–10497.
[38] M.P. Olliff, G. Fischer, Spectrochim. Acta 50A (1994) 2223–2237.
[39] J.T. Houghton, L.G. Meira Filho, B.A. Callander, N. Harris, A. Kattenberg, K. Maskell (Eds.), Climate Change 1995: The Science of Climate Change, Intergovernmental Panel on Climate Change (IPCC), Cambridge University Press, Cambridge, UK, 1996.
[40] G. Myhre, F. Stordal, J. Geophys. Res. 102 (1997) 11181–11200.